

Advanced ponderomotive description of electron acceleration in ICRF discharge initiation

Tom Wauters^{1,*}, Matej Tripský^{1,2}, Anatoli Lysoivan¹, Fabrice Louche¹, Sören Möller³, Riccardo Ragona¹, and Dirk Van Eester¹

¹Laboratory for Plasma Physics, ERM/KMS, 1000 Brussels, Belgium, TEC partner

²Ghent University, Department of Applied Physics, 9000 Ghent, Belgium

³Institute of Energy and Climate Research-Plasma Physics, Forschungszentrum Juelich, Germany - TEC Partner

Abstract. This contribution proposes a new approach for the ponderomotive description of electron acceleration in ICRF discharge initiation. The motion of electrons in the parallel electric field E_z is separated into a fast oscillation and a slower drift around the oscillation centre. Three terms are maintained in the Taylor expansion of the electric field (0th, 1st and 2nd order). The efficiency for electron acceleration by $E_z(z, t)$ is then assessed by comparing the values of these terms at the slow varying coordinate z_0 . When (i) the 0th order term is not significantly larger than 1st order term at the reflection point, or when (ii) the 2nd order term is negative and not sufficiently small compared to the 1st order term at the reflection point, then the electron will gain energy in the reflection.

An example for plasma production by the TOMAS ICRF system is given. Following the described conditions it can be derived that plasma production is (i) most efficient close to the antenna straps (few cm's) where the field gradient and amplitude are large, and (ii) that the lower frequency field accelerates electrons more easily for a given antenna voltage.

1 Introduction

According to Tripský et al. [1], the density evolution in the initial phase of an ICRF discharge can be subdivided into 4 phases characterised by their dominant physics mechanisms. While in later stage (phase III and IV) collective plasma effects are playing an important role, in phases I and II the ionisation rate can be assessed from single electron motions in the antenna vacuum electric field component parallel to the toroidal magnetic field, $E_z(z, t)$. The electron acceleration by $E_z(z, t)$ is described by Lysoivan [2]. The theory separates the motion of charged particles into a fast oscillation and a slower drift around the oscillation centre. Rewriting the velocity and position as $v_z = v_0(t) + v_1(t)$ and $z = z_0(t) + z_1(t)$, the antenna electric field acting on charged particles around the slowly varying coordinate z_0 can be written in a Taylor series expansion:

$$E_z(z = z_0(t) + z_1(t)) = \sum_{n=0}^{\infty} \frac{z_1^n}{n!} \frac{d^n E_z}{dz^n}(z_0). \quad (1)$$

In the work of Lysoivan [2], the Taylor series expansion retains the zeroth- and first-order term. Adding to this theory, for the purpose of this contribution, we introduce as well the quadratic term. Under the condition that z_0 varies slowly, we write two equations of motion representing the

fast (eq. 2) and the slow (eq. 3) dynamics

$$\frac{dv_1}{dt} = -\frac{q_e}{m_e} \left(E_z(z_0) + \frac{z_1^2}{2} \frac{d^2 E_z}{dz^2}(z_0) \right) \cos \omega t \quad (2)$$

$$\frac{dv_0}{dt} = -\left\langle \frac{q_e}{m_e} z_1 \frac{dE_z}{dz}(z_0) \cos \omega t \right\rangle, \quad (3)$$

where $\langle \dots \rangle$ stands for the averaging over the fast oscillation period. The second order term is introduced in the equation of motion of the fast oscillation (eq. 2) as its sign will determine whether the oscillation is focussing around z_0 or defocussing (unstable). From eq. (2) the spatial oscillation amplitude can be derived $\hat{z}_1 = E_z(z_0)q_e/m_e\omega^2$ as well as the minimum electric field value for which the kinetic energy of the oscillating electron overcomes the ionization potential ϵ^{ion} [2]:

$$E_{z,\min} = \frac{\omega}{q_e} \sqrt{2m_e\epsilon^{ion}}. \quad (4)$$

From eq. (3) follows the ponderomotive force responsible for the slow drift of the oscillation centre z_0 with potential [2]:

$$\Phi_p = \left[\frac{q_e E_z(z_0)}{2\sqrt{m_e\omega}} \right]^2. \quad (5)$$

In order to represent with accuracy the electron motion using eq. (2) and (3), the first and second order term need to be smaller than the zeroth and first order term by factor $\xi_{v,1}$ (eq. 6) and $\xi_{v,2}$ (eq. 7) respectively,

*e-mail: t.wauters@fz-juelich.de

$$z_1 \frac{dE_z}{dz}(z_0) < \xi_{v,1} E_z(z_0) \quad (6)$$

$$\frac{z_1}{2} \frac{d^2 E_z}{dz^2}(z_0) < \xi_{v,2} \frac{dE_z}{dz}(z_0), \quad (7)$$

where excursion z_1 can be taken as the amplitude \hat{z}_1 of the zeroth order oscillation. The latter validity conditions are then summarised as

$$\xi_{v,1} > \xi_1 = \frac{q_e}{m_e \omega^2} \frac{dE_z}{dz} \quad (8)$$

$$\xi_{v,2} > \xi_2 = \left(\frac{dE_z}{dz} \right)^{-1} \frac{q_e E_z}{2m_e \omega^2} \frac{d^2 E_z}{dz^2} \quad (9)$$

In the following, single electron simulations will be interpreted in light of the above validity limits.

2 Single electron simulations and interpretations

It is observed in PIC-MCC simulations with code RFdinity1D [1] that upon powering the ICRF antenna, initial electrons present in the torus are quickly expelled from the antenna area. Plasma production by ICRF antennas at typical ICWC pressure levels below $5 \cdot 10^{-4}$ mbar [3] relies therefore on the ability of the E_z profile to change the energy (initial vs. final) of the electrons encountering the antenna area (passing electrons or reflected electrons).

Using a single electron model we investigate the threshold initial energy level ϵ_{tr} above which an electron is able to gain energy from the E_z field. Parametric dependencies on field amplitude E_0 , frequency f and shape σ are investigated. The electric field profile is parametrised as

$$E(z, t) = E_0 \left(e^{-(z-7.5 \text{ cm})^2/\sigma^2} - e^{-(z+7.5 \text{ cm})^2/\sigma^2} \right) \cos(2\pi ft). \quad (10)$$

The single electrons are launched at position z_0 nearby the antenna where $E_z^{RF}(z_0) \approx 0$ with initial energy sampled from a uniform distribution in energy spectrum $\epsilon_0 \in [10^{-1}, 10^2]$ eV and phase $\phi_0 \in [0, 2\pi[$. Each electron is tracked until it has encountered the antenna area 3 times, which corresponds for a 0.5 eV electron in an ASDEX Upgrade size of torus to a duration of about 0.2 ms. The model neglects all collisions. The threshold initial energy ϵ_{tr} is easily obtained by noting the substantial increase in the energy difference between the initial and the final electron energy in the simulation from certain initial energy level on.

Parametric scans for the electric field amplitude (E_0), frequency (f) and shape (σ) are plotted in Figure 1, resp. subfigures a), b) and c). The observed tendencies in these numerical experiments can be interpreted in light of the electric field threshold Eq. (4) and validity limits Eq. (8) and (9).

1. At high electric field amplitude (E_0), low frequency (f) and steep profiles (σ) it is observed that the threshold energy is closely related to the breaking of validity condition eq. (8). The oscillation centre

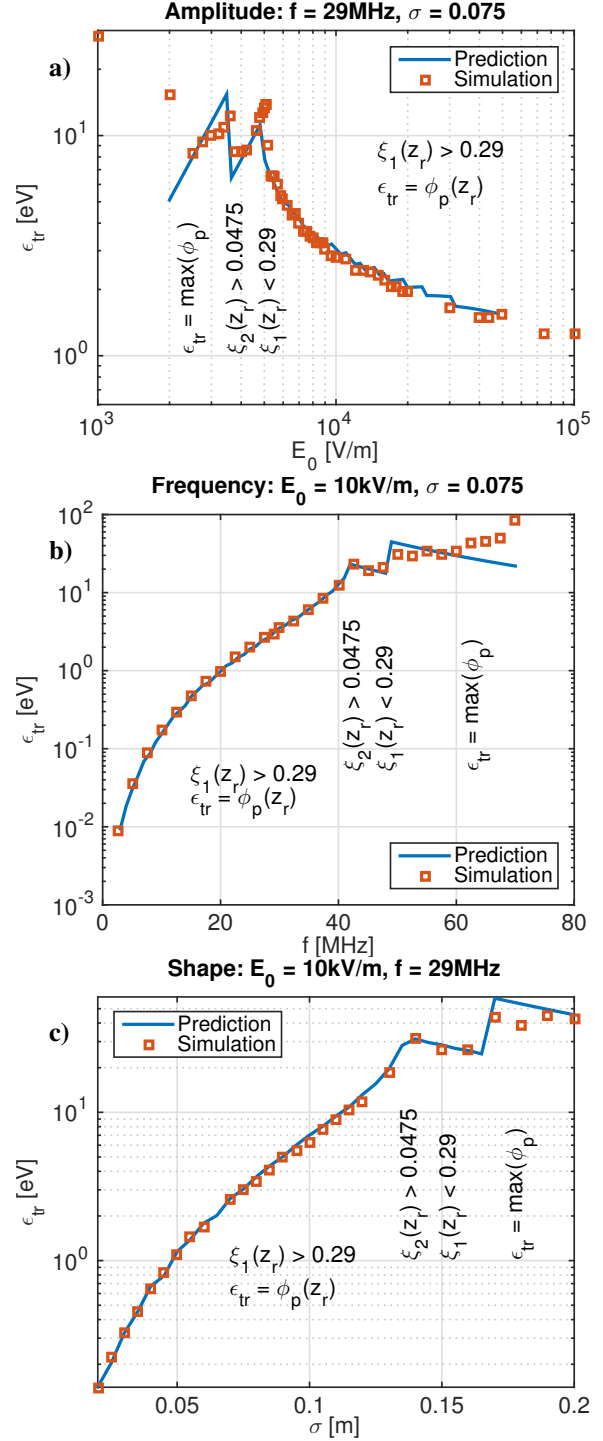


Figure 1. Threshold initial electron energy as function of a) the electric field amplitude (E_0), b) frequency (f) and c) shape (σ) of the parallel electric field (eq. 10). The observed tendencies in the numerical experiments (red rectangles) are result from the electric field threshold Eq. (4) and validity limits Eq. (8) and (9) (blue line)

of an electron that approaches the antenna climbs up the ponderomotive potential (eq. 5). In case the initial electron energy is smaller than the maximum ponderomotive potential $\epsilon_0 < \max(\Phi_p)$, it will be reflected. The initial energy equals the final energy ($\epsilon_0 \approx \epsilon_f$) as long as $\xi_1 < \xi_{v,1} \approx 0.29$ at the reflection point z_r . The electron was found to acquire energy from the vacuum electric field in case $\xi_1 > \xi_{v,1}$ at the reflection point. The reflection point corresponds to the location where the initial energy equals the ponderomotive potential ($\Phi_p(z_r) = \epsilon_0$). The threshold energy ϵ_{tr} can therefore be taken as the ponderomotive potential at the location where $\xi_1 = \xi_{v,1}$.

2. When validity limit eq. (8) is fulfilled for the entire electric field shape at the antenna edge ($\xi_1 < \xi_{v,1}$), i.e. at intermediate E_0 , f and σ , then the threshold energy ϵ_{tr} is determined by validity limit eq. (9). The single electron simulations showed that the final energy after reflection may differ from the initial energy as soon as the oscillation centre enters the area with negative second order term. This is understood from eq. (3); a positive second order term focusses the oscillating electron around the slowly varying coordinate, while a negative second order term leads to an unstable oscillation (defocussing). The initial energy equals the final energy ($\epsilon_0 \approx \epsilon_f$) as long as $\xi_2 < \xi_{v,2} \approx 0.0475$ at the reflection point z_r . The threshold energy ϵ_{tr} approximates the ponderomotive potential at the location where the second derivative of the electric field profile turns negative.
3. When both conditions (eq. 8 and 9) are fulfilled, then ϵ_{tr} is determined by the maximum ponderomotive potential. Only electrons with initial energy larger than the ponderomotive potential $\epsilon_0 > \max(\Phi_p)$ are able to enter into the antenna area and eventually to gain energy.
4. At low E_0 , high f or high σ , the electrons are unlikely to gain sufficient energy for ionisation in interaction with the vacuum electric field regardless of their initial energy (eq. 4).

3 Assessment of TOMAS ICRF vacuum electric field for plasma production

The above derived and studied set of conditions for electron acceleration by the parallel vacuum electric field in toroidal devices allows to pre-assess the ability for any ICRF antenna geometry, phasing, input power and frequency to initiate plasma as function of, e.g., the radial coordinate R . An example for the TOMAS ICRF system [4] is shown in figure 2 for an input voltage of 1.5 kV, corresponding to ~ 3 kW of forward RF power. Sub-plot 2(a) shows the maximum amplitude of the E_z field for RF frequencies in range $f = 15$ MHz to 45 MHz, together with the minimum amplitude required for accelerating electrons above the ionisation potential (horizontal

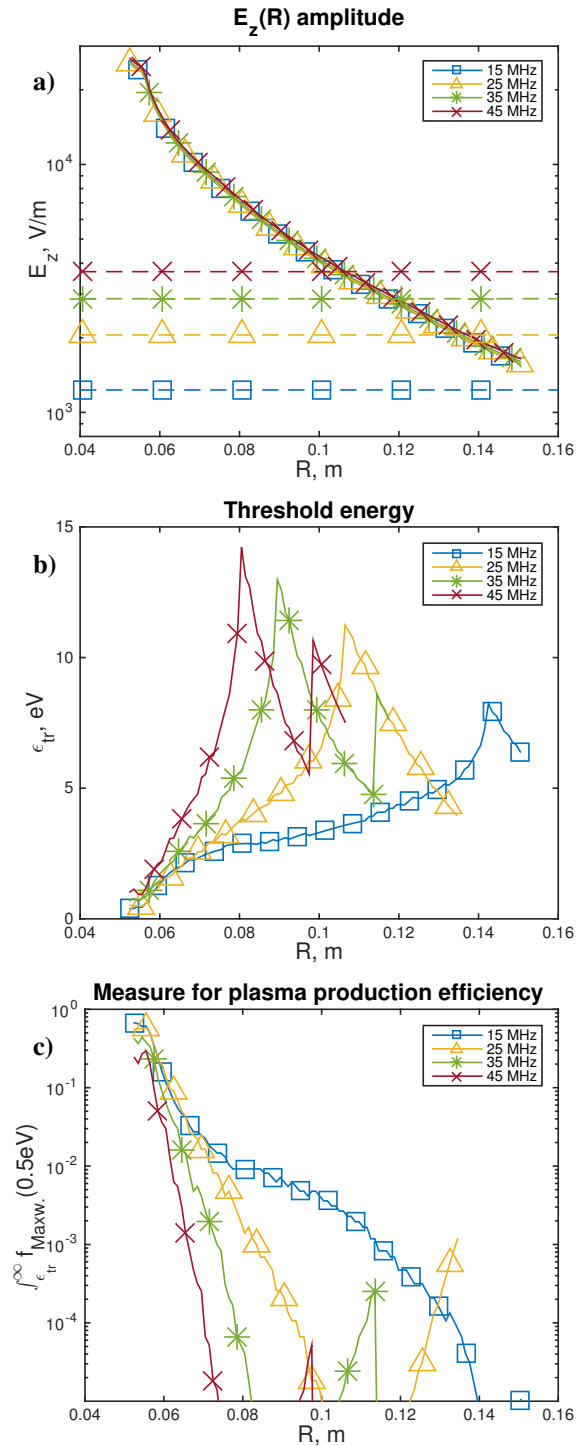


Figure 2. Illustration of dependencies as function of radius R for TOMAS ICRF antenna. E_z fields are obtained in the horizontal midplane using the commercial electromagnetic software CST Microwave Studio®.

lines as given by eq. (4)). The curves in sub-plot 2(b) and 2(c) are discontinued at radial positions where the E_z amplitude becomes lower than this minimum. The antenna box face is located at 5.5 cm.

Sub-plot (b) shows the threshold energy as derived from the validity conditions. The threshold energy is minimum close to the antenna straps where the field gradient

is steepest and largest in amplitude. The threshold energy, at first determined by validity condition eq. (8) ($\xi_1 < \xi_{v,1}$), increases to reach a maximum further in the torus (e.g. at 8 cm for 45 MHz). Beyond this point the threshold energy is determined by condition eq. (9) ($\xi_2 < \xi_{v,2}$) and decreases until a second discontinuity occurs (e.g. at 9.9 cm for 45 MHz). Beyond this point both validity limits are fulfilled and the threshold energy is determined by the maximum ponderomotive potential.

Sub-plot (c) shows the fraction of electrons in a Maxwellian energy distribution of 0.5 eV that has energy above the threshold energy ϵ_{tr} . It provides a measure for the efficiency for accelerating a population of low temperature electrons that are initially present in the vessel. From this picture it is clear that the efficiency drops dramatically by 4 orders of magnitude over a distance where the threshold energy increases by only one order of magnitude. From this analysis it can therefore be concluded that plasma production in the vacuum E_z -field of poloidal ICRF antenna straps inside an antenna box occurs in the vicinity (few cm's) of the antenna box. Moreover it can be concluded that plasma production is more efficient at low frequencies than at high frequency for a given strap voltage (1.5 kV).

4 Conclusion

The majority of the electrons in the initial phase of an ICRF discharge reside outside of the antenna area and, in order to overcome the ionisation potential, need to gain energy via interaction with the vacuum parallel electric field that locates in the vicinity of the antenna. It is found that electrons with initial energy smaller than the maximum ponderomotive potential may gain energy in reflections at the sides of the antenna. This contribution proposes hereto an advanced ponderomotive description of electron acceleration. The motion of the electrons in the parallel electric field E_z is separated into a fast oscillation and a slower drift around the oscillation centre. Three terms are maintained in the Taylor expansion of the electric field, namely the 0th, 1st and 2nd order term. The efficiency for electron

acceleration by $E_z(z, t)$ is then assessed by comparing the values of these terms at the slow varying coordinate z_0 at the antenna outer edges. When (i) the 0th order term is not significantly larger than 1st order term at the reflection point, or when (ii) the 2nd order term is negative and not sufficiently small compared to the 1st order term at the reflection point, then the electron will gain energy in the reflection. (iii) Electrons with initial energy larger than the maximum ponderomotive potential will enter into the antenna area. Finally (iv) the 0th order term gives the minimum electric field amplitude that accelerates an electron above the ionisation potential within a fast oscillation period.

An example for plasma production by the TOMAS ICRF system [4] is given. Following the described conditions it can be derived that plasma production is (i) most efficient close to the antenna straps (few cm's) where the field gradient and amplitude are large, and (ii) that the lower frequency field accelerates electrons more easily for a given antenna voltage.

Acknowledgements

This work has been carried out within the framework of the EUROfusion Consortium and has received funding from the European research and training programme under grant agreement N 633053. The views and opinions expressed herein do not necessarily reflect those of the European Commission.

References

- [1] Tripský M et al, 2017, *Nucl. Fusion* at press: <https://doi.org/10.1088/1741-4326/aa8446>
- [2] Lysoivan A et al, 2012 *Plasma Phys. Control. Fusion* **54**, stacks.iop.org/PPCF/54/074014
- [3] Wauters T et al, 2015, *J. Nucl. Mater.* **463**, <http://dx.doi.org/10.1016/j.jnucmat.2014.12.097>
- [4] Louche F et al, 2017, *Fusion Eng. Des.*, in press: <https://doi.org/10.1016/j.fusengdes.2017.04.123>